Arch. Metall. Mater. **71** (2026), 1, 253-261

DOI: https://doi.org/10.24425/amm.2026.157786

N. KHAMROEV[1*], I. EGAMBERDIEV[1], KH. ASHUROV[1]

EFFECT OF CHROMIUM CONTENT AND HEAT TREATMENT CONDITIONS ON THE STRUCTURE OF WEAR-RESISTANT WHITE CAST IRONS

In this study analyzed, the effects of heat treatment on the structure of white cast iron with different chromium contents (28 wt.%Cr to 32 wt.%Cr). To observe changes in the structure and increase its wear resistance, the cast materials were heat treated. The heat treatment was carried out in the following order: (1) quenching: two samples of each material were kept in the temperature range of 1000°C for 1 hour and cooled with oil (QT(o)) and forced air cooling (QT(f.a.c.)), (2) tempering at a temperature of 200°C for 2 hours were kept and cooled under the influence of room temperature (QT(c.r.t)). In addition, in order to study the microstructure of the cast samples and compare their state after the heat treatment process, the samples obtained from each material were not subjected to treatment (AC). The microstructures of the materials were analyzed using scanning electron microscopy (SEM), and the dimensions of the structural constituents were further processed using the ImageJ software. The obtained results show that the microstructure of the samples obtained in the as-cast state mainly consists of primary carbides such as M_7C_3 and $M_{23}C_6$ and an austenitic matrix. As a result of heat treatment, the metal matrix transformed from austenite to martensite, retained austenite phases remained, and at the same time, secondary carbides were precipitated throughout the matrix. Among the analyzed materials, the best characteristics were demonstrated by the heat-treated and oil-cooled sample with a Cr content of 31%. The second sample with a Cr content of 28% showed the worst wear resistance in the as-cast condition.

Keywords: White cast iron; heat-treatment; abrasive wear; casting

1. Introduction

High-chromium cast irons are widely used as wear-resistant materials in the mining industry, cement production, and metallurgy. Typically, these alloys are based on iron and carbon, containing 12-32% Cr and 2.0-3.5% C [1-4]. A chromium content in the range of 26-30% promotes the formation of eutectic carbides in a high fraction within the structure, which ensures superior resistance to abrasive wear during rock comminution processes. Their microstructure consists of a metallic matrix and carbides, where the matrix may be austenitic, ferritic, pearlitic or martensitic. Eutectic carbides of the M_7C_3 and $M_{23}C_6$ types are usually present, while hard phases such as M_6C, MC, and M_2C can also form depending on the heat treatment and solidification conditions [5,6]. When high-chromium cast iron is poured, solidification initially proceeds through the formation of austenitic dendrites. During crystallization, eutectic carbides-mainly of the M_7C_3 and $M_{23}C_6$ types precipitate between the dendrites in a prismatic and lamellar morphology. Upon subsequent cooling, part of the austenite, which is stable only at elevated temperatures, undergoes transformation into the martensitic phase [3,7].

A number of studies have been conducted by researchers to improve the mechanical properties of high-chromium wear-resistant cast irons. To achieve this goal, various approaches have been applied and are still being developed. These include the addition of alloying elements or increasing the content of existing ones, the optimization of heat treatment technologies, as well as the control of grain boundaries through mechanical and ultrasonic methods [8-10]. Among these approaches, the most widely applied and economically efficient are the modification of the chemical composition through the addition of various alloying elements and the application of heat treatment processes. To improve the wear resistance of high-chromium cast irons, extensive research has been devoted to the addition of alloying elements such as vanadium, molybdenum, tungsten, and titanium. These alloying elements exhibit a strong affinity for carbon, enabling them to form individual carbides – such as Mo_2C, WC, and TiC – as well as participate in the development

[1] NAVOI STATE UNIVERSITY OF MINING AND TECHNOLOGIES, MECHANICAL ENGINEERING AND MATERIAL SCIENCE, DEPARTMENT OF LOCALIZATION OF INDUSTRIAL PRODUCTION, GALABA 76V, 210100, NAVOI, UZBEKISTAN

* Corresponding author: nurbek.hamroyev@nsumt.uz

of complex carbide phases together with chromium and iron. The presence of such carbides significantly enhances the hardness and thermal stability of the alloy, while also contributing to improved resistance against abrasive and impact wear [11,12].

However, due to their scarcity and high cost, the addition of these elements and the corresponding research processes become rather complex. Alongside the above-mentioned elements, manganese is also introduced as an alloying element in wear-resistant cast irons. Unlike molybdenum, tungsten, or titanium, manganese does not form its own carbides; instead, it plays a key role in stabilizing the austenite phase and adversely affects the hardness of the matrix, thereby reducing the wear resistance of materials [13].

For this reason, the present study focused on enhancing the wear resistance of the material primarily through the utilization of existing alloying elements, with chromium selected as the key alloying component. At a Cr/C ratio of 10, chromium plays a decisive role in the formation of primary and eutectic carbides (M_7C_3 and $M_{23}C_6$), while also promoting the development of M_6C carbides instead of M_2C carbides [14]. In addition, heat treatment techniques aimed at obtaining a martensitic structure and promoting the formation of secondary carbides along the metallic matrix have also been investigated as an effective means of increasing material hardness. Among the different approaches, quenching is generally considered the most efficient method for hardness improvement. This process is typically carried out within the temperature range of 800-1050°C, based on phase diagram considerations, followed by rapid cooling in oil, air, or water. To relieve the internal stresses induced by quenching, a subsequent tempering treatment is applied, usually in the range of 200-250°C. The refinement of structural component size and distribution, achieved via alloying and heat treatment, is a key factor in improving the wear resistance of white cast iron.

2. Methodology

2.1. Material and methods

The chemical composition of the studied samples is presented in TABLE 1.

TABLE 1

Chemical composition of samples (mass %)

No	C	Si	Mn	Cr	Mo	Ni	Cu	B	Fe
1	2.62	1.00	0,54	31.06	0.10	1.56	0.89	0.006	Ball.
2	2, 58	1.08	0.52	27.98	0.12	1.29	0.30	0.006	Ball.

To cast the samples, 10 kg of cast iron from each material was melted in high-frequency induction furnaces at a temperature of 1480°C and poured into a sand mold. To test the wear resistance, 10×10×100 mm^3 and Ø20×100 mm^3 and Ø20×100 samples were cut from the bottom of the molds (20×20×100 mm^3 and Ø20×100 mm$_)$, the surface was ground on a FORCIPOL 1V automated grinding machine and polished with a silicon oxide suspension (0.05 μm). To observe changes in the structure and increase its wear resistance, the cast materials were heat treated in Daihan Scientific furnaces. The heat treatment was carried out in the following order (Fig. 1): (1) quenching: two samples of each material were kept in the temperature range of 1000°C for 1 hour and cooled with oil (QTo), (2) tempering at a temperature of 200°C for 2 hours were kept and cooled under the influence of room temperature (QTc.rt). In addition, in order to study the microstructure of the cast samples and compare their state after the heat treatment process, the samples obtained from each material were not subjected to treatment (AC).

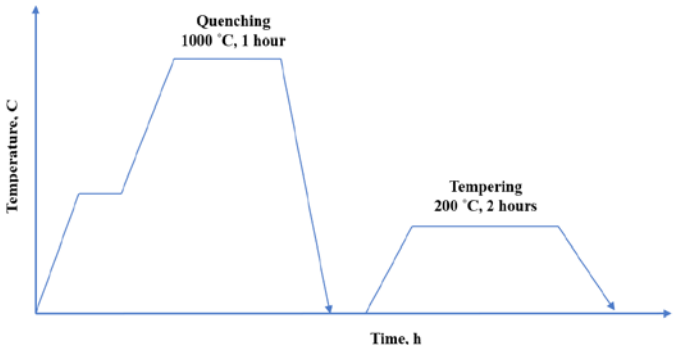

Fig. 1. Heat treatment conditions

A Tescan Vega 3 SBH scanning electron microscope was used to observe the microstructure of the materials. The mechanical properties were tested using Wilson Rockwell 574. In this study, the abrasive wear performance of the material was determined using the test scheme shown in Fig. 2. The sample was placed between a rotating wheel and a holder, and a flow of quartz sand with an average diameter of 300 mm and a hardness of 1000 HV was passed between them at an impact speed of 4.2 g/s for 360 seconds. The abrasive wear results were

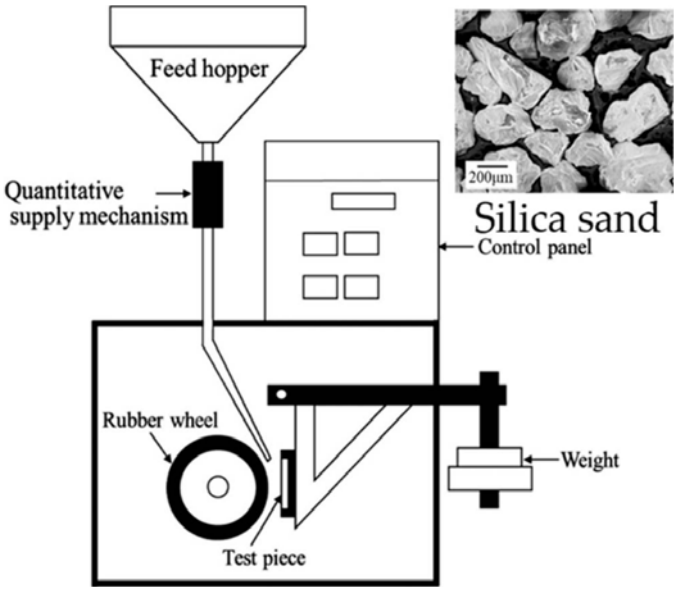

Fig. 2. Schematic diagram of the abrasive testing apparatus

determined by measuring the mass of the material after working for the above time. Data processing and graphical analysis were carried out using Origin Pro software, whereas ImageJ software was used for the measurement and characterization of phase dimensions within the microstructures. The analysis and construction of the alloys' phase diagrams were performed using Thermo-Calc software.

3. Results and discussion

The results obtained by scanning electron microscope SEM, EDS of the samples are shown in Figs. 4-6. Fig. 4 shows the microstructure of sample No. 1 after casting and after heat treatment according to the chemical composition given in TABLE 1. The image (4a) shows that the base metal has large grains, and smaller carbides such as MC, $M_{23}C_6$ and M_7C_3 are scattered around it [15]. This result is consistent with the structural components predicted in the Fe-C-Cr phase diagram. Several researchers worked on the crystallization conditions of alloys and the formation of metallic bases and carbides in them, and finally the results were summarized by Tabrett et al. [16]. According to the conclusions, the crystallization process occurs with the formation of austenite dendrites. As the temperature decreases, the residual liquid phase approaches the eutectic temperature, consisting of M_7C_3 and austenite. Subsequently, the temperature equal to the ambient temperature leads to the preservation of metastable austenite. This is explained by the presence of a large number of alloying elements and carbon, which leads to the formation of pearlite in the structure and a drop in the formation temperature of general martensite below zero [17].

The dark phases visible in the second image (4b) are carbides of arbitrary shape and size. The carbides are quite large and have different shapes, indicating different growth conditions. We can see that these types of carbides are usually M_7C_3 or $M_{23}C_6$ type carbides. Their size and uneven distribution, rapid growth of carbides indicates a strong effect of heat treatment. Such a structure may increase the difficulty of machining, but under abrasive wear conditions, M_7C_3 carbides with a cross section parallel to the wear surface show excellent resistance.

In the microstructure after heat treatment, secondary carbides can be seen that form on the surface of the metal base. Their types depend on the alloying elements added. This helps to act as a barrier between the surface and the material.

In the study of alloys, the design process plays a crucial role. Below are the phase diagram analyses of the investigated alloys obtained using the Thermo-Calc software (Fig. 3). In these figures, the carbon content is considered as a variable, while the remaining alloying elements are fixed according to the selected composition. It can be observed that the phase diagrams reveal certain similarities. The phases and their types, which evolve with changes in temperature ranges and carbon content, are presented separately in each diagram.

In both diagrams, it can be observed that the metallic matrix consists of austenite and ferrite, while the primary carbides formed are $M_{23}C_6$ and M_7C_3. The type of metallic matrix phase depends on the solidification conditions. Depending on the heat treatment environment and temperatures, in addition to the primary carbides, secondary carbide phases may also form along the surface of the metallic matrix. These secondary carbides are not represented in the phase diagrams but can be identified through microstructural analysis.

Based on the Fe-C-Cr phase diagram (Fig. 3), it can be said that the microstructure of castings obtained from this type of white cast iron consists of eutectic carbides, ferrite and austenite [18]. The microstructures (Figs. 4-6) represent a hypoeutectic composition consisting of eutectic carbides and primary austenite dendrites. According to researchers [19], the matrix of high-chromium white alloy cast iron usually changes from austenite to martensite during heat treatment. However, a small amount of residual austenite can be found in the microstructure even after heat treatment.

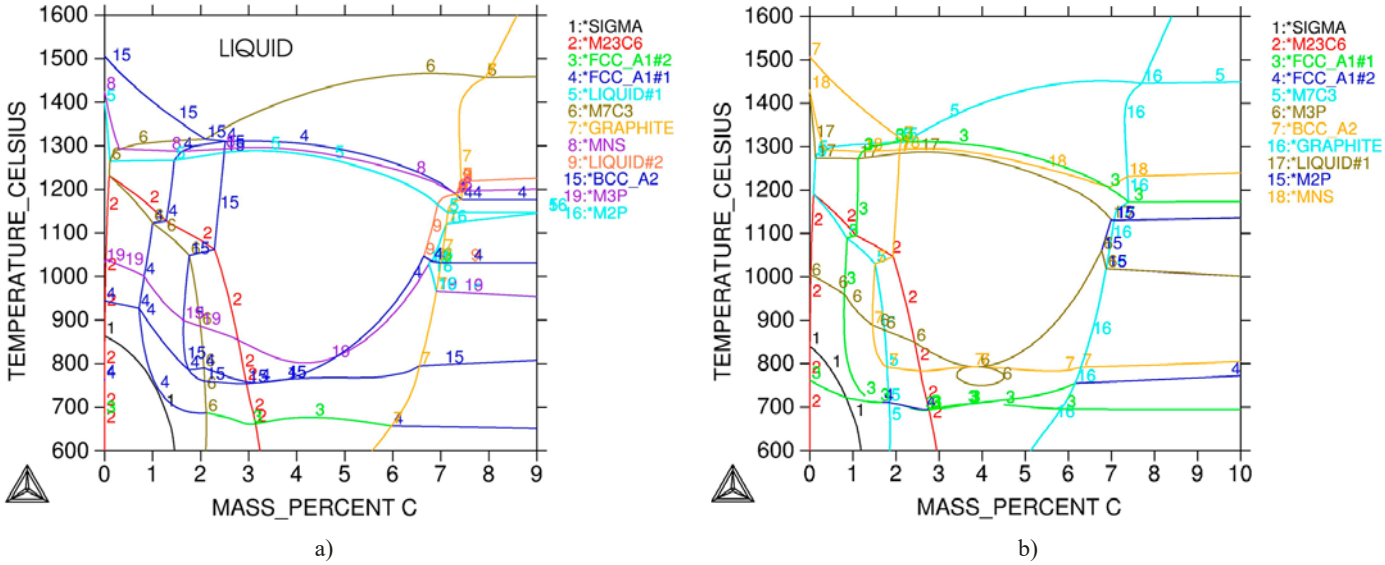

a) b)

Fig. 3. Phase diagrams based on the Fe-C-Cr system. a) alloy No. 1. b) alloy No. 2

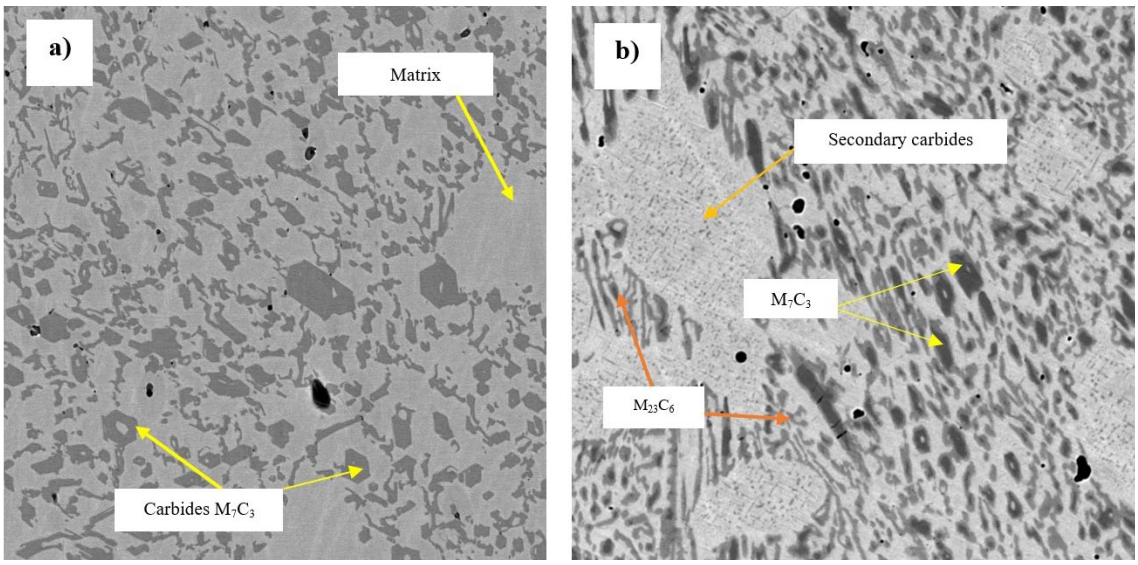

Fig. 4. Microstructure of alloy No. 1. a) in the cast state, b) heat-treated, cooling medium after heat treatment – oil

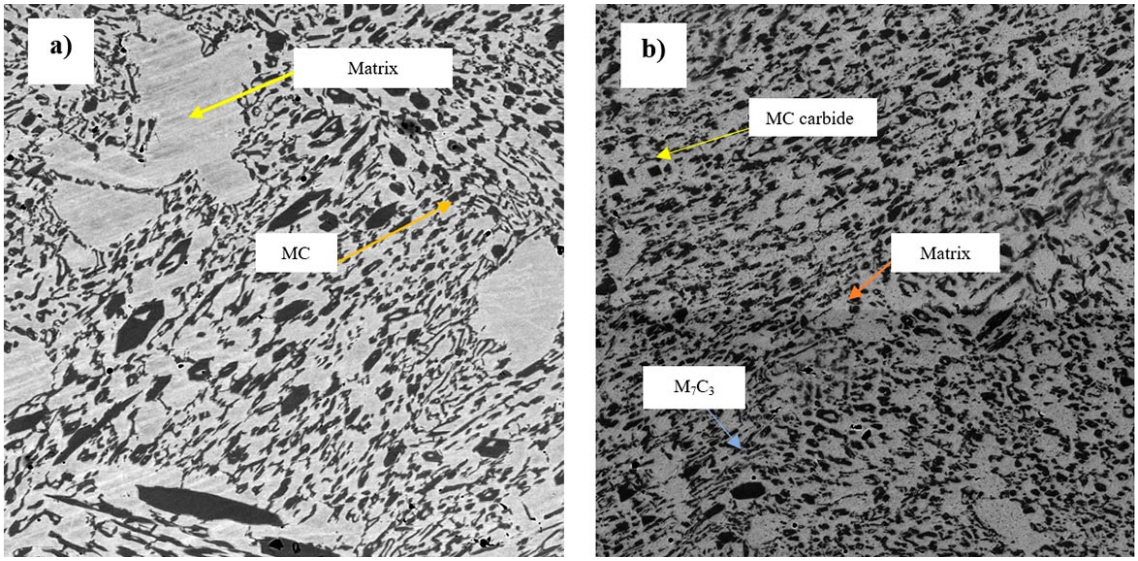

Fig. 5. Microstructure of alloy No. 2. a) as cast, b) heat-treated, cooling medium after heat treatment – oil

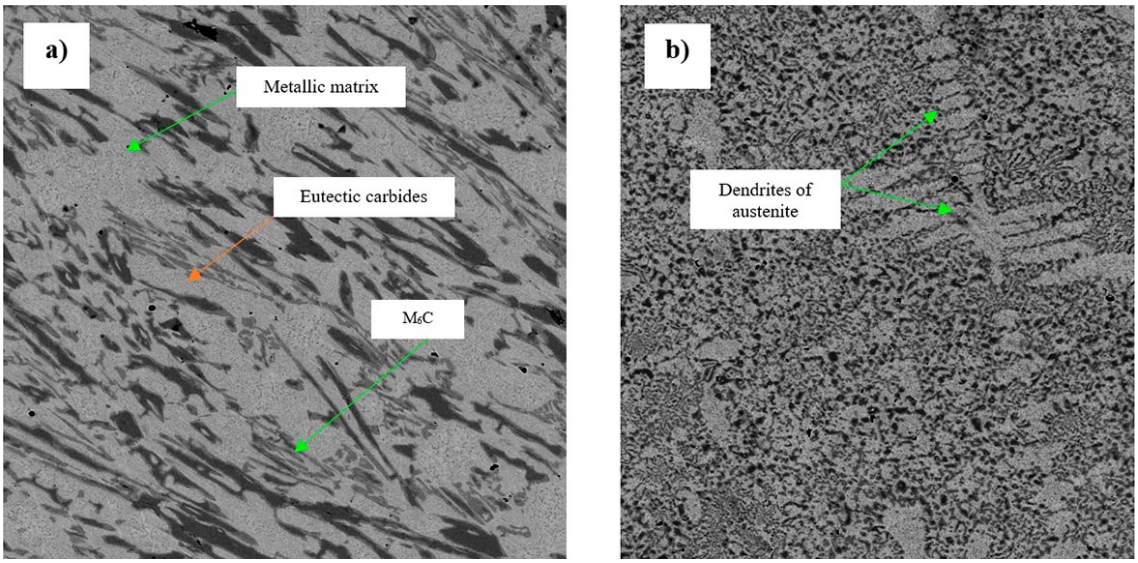

Fig. 6. Microstructures of alloys after heat treatment. a) No. 1. b) No. 2. Cooling medium – air

According to Yilmaz [20] and others, the property of materials with significant resistance to abrasive wear is achieved due to high hardness, but in some cases, control of residual austenite in the metal base after heat treatment serves to achieve a sufficient level of strength. In addition, the high resistance of white cast irons with a high chromium content to abrasive wear can be due to the formation of special carbides in the structure, uniformly and dispersed over the surface of the metal base. From the microstructures obtained using SEM, it is evident that a sufficient number of carbides are highlighted in all images.

Regardless of the amount of Mn, Mo and Ni in the alloys, carbide M_7C_3 was precipitated in all samples. Since the atomic radius of Mn and Cr is close to the radius of Fe, they occupy a position replacing iron in the crystal lattice of the formed carbide. Manganese is a carbide-forming element, in addition, it dissolves in austenite to the solubility limit, and the remaining part serves to precipitate carbides of the M_7C_3 type and does not form its own carbide [19]. The microstructure shown in Fig. 4a) shows that the sizes of the structural components after casting and the areas of austenite dendrites are large.

The EBSD (Electron Backscatter Diffraction) analysis results obtained by scanning electron microscopy are presented in Fig. 7a). According to the phase diagrams of the alloys, it is recognized that mainly M_7C_3 and $M_{23}C_6$ carbides are formed in their microstructure. However, according to these microstructural analysis results, in the microstructures of the as-cast sample No. 1, a very small amount of BCC phase at the grain boundaries and (presumably) secondary CrC carbides formed in the metal matrix can also be observed. The formation of these secondary precipitates may be related to rapid solidification conditions. The quantitative phase analysis revealed that the microstructure of the studied sample consists predominantly of FCC iron (62.43%), with smaller fractions of BCC iron (3.99%). Among the carbide phases, Cr_7C_3 constitutes 30.09%, CrC 2.64%, and $Cr_{23}C_6$ 0.85% of the volume. These results indicate a microstructure dominated by austenite with significant primary and secondary

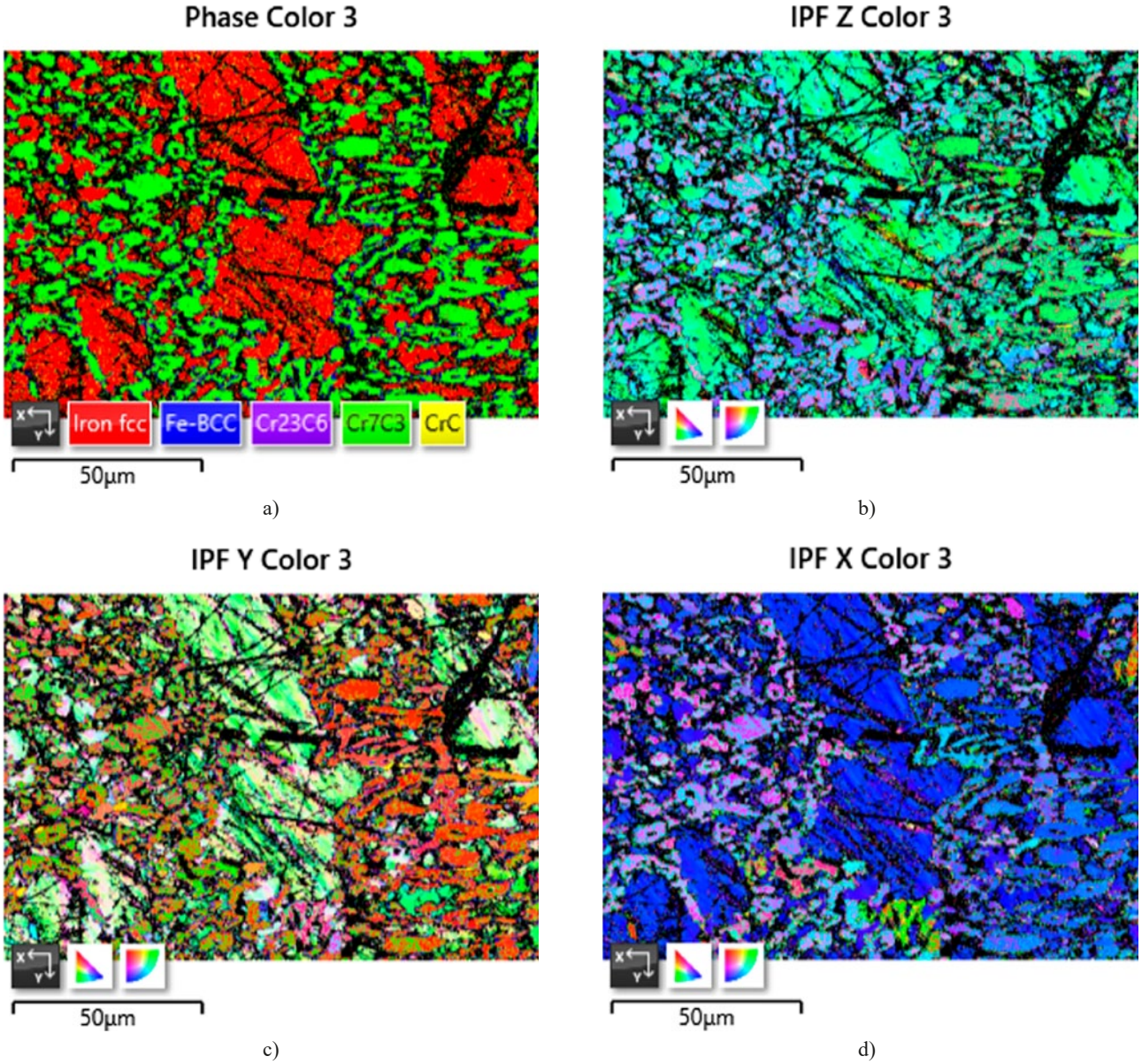

Fig. 7. EBSD analysis (a) and crystallographic orientation of grains (b), (c), and (d)

carbide precipitations, which are expected to strongly influence the material's hardness and wear resistance.

The microstructural images acquired by SEM were further analyzed with ImageJ software to determine the size distribution of the surface-dispersed phases (carbides/dendrites). For Sample No 1 in the as-cast condition, the average phase size was relatively small (Mean ≈ 2.007 μm^2), while the distribution was highly dispersed (SD = 21.870 μm^2), indicating the coexistence of both very fine (Min = 0.072 μm^2) and extremely coarse phases (Max = 762.066 μm^2). These indicators may depend on the crystallization process. After heat treatment followed by oil quenching, the mean phase size slightly increased (2.268 μm^2), but the distribution range became narrower (SD = 14.057 μm^2, Max = 258.327 μm^2), which suggests partial homogenization of the microstructure. In contrast, air cooling led to a lower mean size (1.339 μm^2) but with the widest distribution range (SD = 25.530 μm^2, Max = 1430.440 μm^2), implying the formation of larger secondary carbides along the matrix boundaries. For Sample No 2 in the as-cast state, the mean phase size was significantly larger (18.337 μm^2), accompanied by a broad distribution (SD = 52.544 μm^2, Max = 934.368 μm^2). After heat treatment with oil quenching, the mean size decreased considerably (4.591 μm^2), and the distribution narrowed (SD = 19.118 μm^2, Max = 450.532 μm^2), pointing to the refinement of carbides. When cooled in air, the mean size was reduced further to 2.177 μm^2 with a very limited distribution range (SD = 6.837 μm^2, Max = 167.548 μm^2), which indicates that slow cooling promoted a more uniform dispersion of phases compared to the as-cast state.

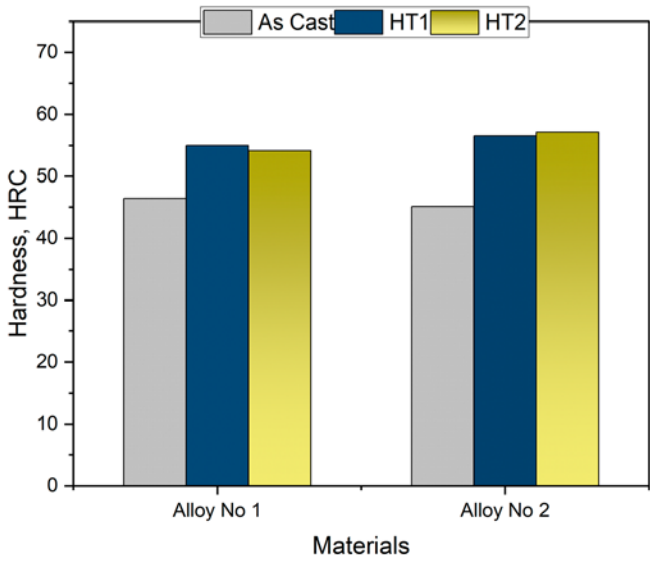

Fig. 8. Hardness of materials in the as-cast state and after heat treatment

Fig. 8 presents the hardness values of the materials in both the as-cast condition and after heat treatment. In the as-cast state, the hardness of Sample 1 (54HRC) is higher compared to Sample 2 (50HRC), which can be attributed to the higher chromium content and the formation of carbides due to the interaction of Cr and C. After heat treatment followed by quenching in oil, the hardness values of the samples show almost no significant difference. This is explained by the sufficient formation of carbides in both samples and their relatively uniform dispersion within the matrix. In addition, according to the hardness of the alloys and SEM images, it can be noted that, along with martensite, residual particles of austenite are present in the metal base.

After heat treatment followed by air cooling, the EDS analysis of the phase constituents was performed for Sample 1 (Fig. 9). The elemental composition and their relative fractions in the corresponding phases are presented in detail in TABLE 2. The microstructural analysis revealed the presence of both primary and eutectic carbides, distinguished by their darker and lighter contrast, respectively, while secondary carbides were observed precipitating along the matrix surface. Energy-dispersive X-ray spectroscopy (EDS) analysis.

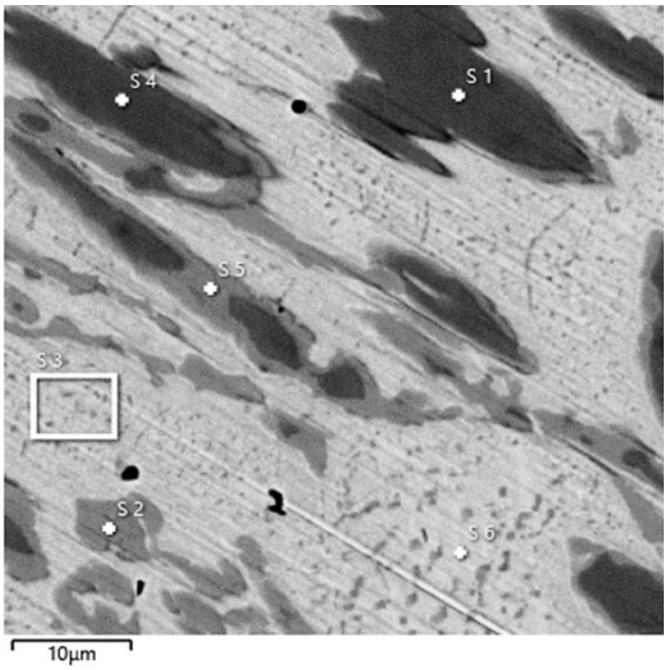

Fig. 9. Spectral analysis of alloy No. 1

TABLE 2

Elemental distribution in spectra (mass %)

Spectrum Label	C	Si	Cr	Mn	Fe	Ni	Cu	Total
S 1	12.67		67.14		20.19			100
S 2	9.15		58.62		31.7	0.53		100
S 3		1.34	23.43		73.03	2.2		100
S 4	12.78		67.01		20.2			100
S 5	9.38		58.28		31.74	0.59		100
S 6		1.23	20.18	0.47	74.8	2.43	0.89	100

The distribution and states of each added chemical element are shown in Fig. 10, which shows the EDS results. In order to determine the chemical composition of the metal base and carbides located on the surface, a heat-treated and oil-cooled sample of alloy 1 was obtained by point and volume analysis using EDS and SEM methods. To ensure the reliability of the results, the

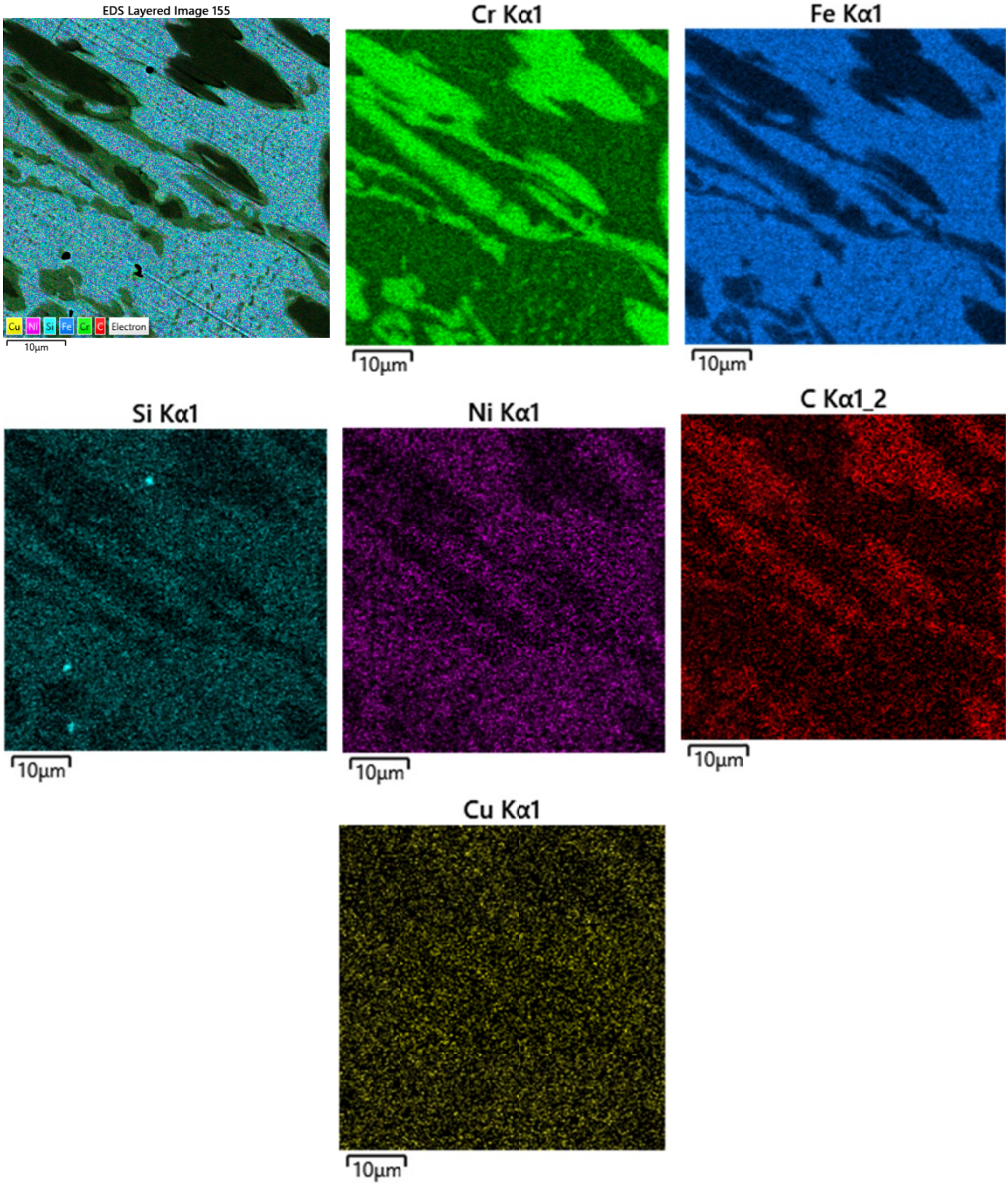

Fig. 10. Distribution of chemical elements in the microstructure of chromium content Cr 31% material according to SEM-EDS analysis

analyses were carried out 5 times from different points on the sample surface, the results are presented in TABLE 2. The image shows that the spectra S1 and S4 are separated by dark color and C (12.67%), Cr (67.14%), Fe (20.19%) are shown as the main elements. There are high concentrations of carbon and chromium in this spectrum. The spectra S2 and S5 are lighter compared to the above-mentioned phases, and the elements C (9.15%), Si (58.62%), Fe (31.7%) are high, and Ni is also found in small amounts in this phase. The S3 and S6 spectra show a metallic matrix, the main elements of which are C (1.34%), Cr (23.43%)

and Fe (73.03%). At this site, iron is highly concentrated and chromium is relatively low. The appearance of small amounts of Cr may be due to the formation of secondary carbides, and the abundance of Fe may indicate an iron-based phase, possibly martensite or austenite [21].

Wear characteristics. During the crystallization process in multi-component high-carbon cast irons, prismatic or rhombic carbides M_7C_3 and lamellar carbides $M_{23}C_6$ are may be formed. According to the Thermo-Calc program, carbides M_7C_3 and $M_{23}C_6$ are formed in the eutectic state, but according to the phase diagrams associated with the practice of scientists, multi-component white cast iron has a basic chemical composition that begins to harden due to the crystallization of primary austenite [22]. Then, carbide M_7C_3 is formed as the first eutectic, and then carbide $M_{23}C_6$ is formed as the secondary or final eutectic. Carbide MC retains its shape in the structure of the cast part in annealed samples, but carbides M_2C are absent in the annealed samples. Instead, the M_6C carbide is formed together with the M_7C_3 and MC carbides in configurations similar to the M_2C phase shape. In this paper, this is explained by the formation of M_7C_3 carbides at the boundaries of the metal base and $M_{23}C_6$ as a result of increasing the heat treatment temperature. During wear testing, the samples exhibited the following wear behavior. In the as-cast condition, the wear rate of Sample 1 was nearly twice that of Sample 2. This behavior is explained by the fact that the metallic matrix is fully austenitic in this structure and eutectic carbides have formed, acting as a barrier to wear. Among the heat-treated specimens, the sample with 31 wt.% Cr that was oil-quenched demonstrated the best wear resistance. In contrast, cooling Sample 2 by air flow after heat treatment produced the poorest wear performance among the heat-treated samples. This phenomenon shows that the hardness of materials is not always proportional to their abrasive wear indices. In high-chromium or multi-component wear-resistant cast irons, the metallic matrix is typically austenitic, and under heat treatment the austenite partially transforms into martensite.

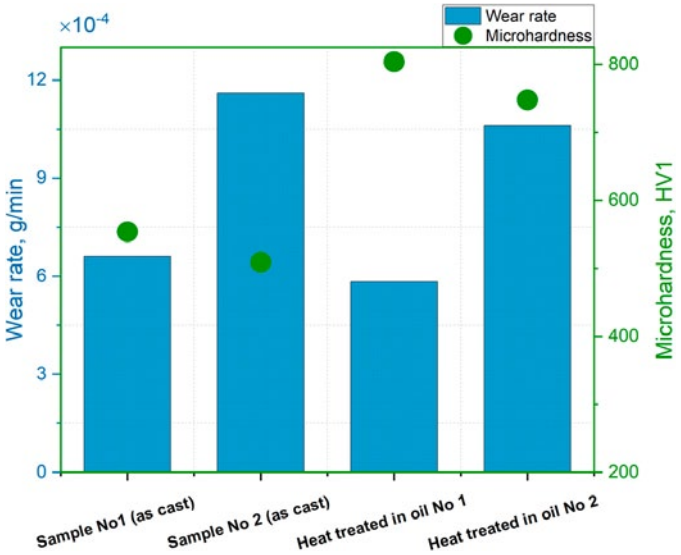

Fig. 11. Correlation between abrasive wear and microhardness of materials

In the present study, the austenitic matrix was observed to have partially transformed into martensite. This transformation is also reflected in the hardness and microhardness measurements. The microhardness results show that Sample 1 in the as-cast state exhibited 554 HV1, while Sample 2 showed 509 HV1. After heat treatment and oil quenching, these values increased to 804 HV1 and 748 HV1, respectively. This phenomenon is associated with the reduction of carbon content in the matrix during tempering, caused by the precipitation of secondary carbide phases. The correlation between wear test results and microhardness parameters indicates that, with increasing microhardness, the degree of wear progressively decreases (Fig. 11).

4. Conclusion

In this study, abrasion tests were conducted on heat-treated wear-resistant white cast iron with high chromium content in different amounts. Based on the above results and analysis, the following conclusions were drawn:

1. The microstructure of the wear-resistant cast iron with 31% Cr and 2.6% C is dominated by an austenitic matrix (62.43%), with minor ferrite at grain boundaries (3.99%) and a significant fraction of primary prismatic Cr_7C_3 carbides (30.09%). Secondary carbides, including $Cr_{23}C_6$ (0.85%) and CrC (2.64%), are also present, indicating a microstructure that combines high austenite content with reinforcing carbide precipitations, which is expected to enhance hardness and wear resistance.
2. The heat-treated microstructure consists of a metal matrix composed of martensite and retained austenite, along with eutectic and secondary carbide phases. Furthermore, quenching with air cooling leads to a non-uniform metal matrix, resulting in a dendritic morphology.
3. An increase in chromium content leads to an enhancement of the hardness and microhardness of the alloy. This effect is primarily attributed to the formation of chromium–carbon carbides and the corresponding increase in their volume fraction.
4. The first sample with a high chromium content (31.06% Cr, 2.62% C) exhibited the lowest wear rate in all conditions. In particular, the heat-treated and oil-quenched material demonstrated the best tribological behavior across all tested conditions.

REFERENCES

[1] K. Holmberg, P. Kiviktyo-Reponen, P. Harkisari, K. Homberg, Global energy consumption due to friction and wear in the mining industry. Tribol. Int. **115**, 116-139 (2017). DOI: https://doi.org/10.1016/j.triboint.2017.05.010

[2] K. Holmberg, A. Erdemir, Influence of tribology on global energy consumption, costs and emissions. Friction. **5** (3), 263-284 (2017). DOI: https://doi.org/10.1007/s40544-017-0183-5

[3] M.E. Garber, Iznosostoykie belie chuguni: Svoystva, struktura, texnologiya, ekspluatatsiya, 2010 Mashinostroeniya, Moskva.

[4] K. Kusumoto, K. Shimizu, X. Yaer, Y. Zhang, Y. Ota, J. Ota, Abrasive wear characteristics of Fe-2C-5Cr-5Mo-5W-5Nb multi-component white cast iron. Wear **367-367**, 22-29 (2017). DOI: https://doi.org/10.1016/j.wear.2017.01.096

[5] L. Xu, F. Wang, M. Li, X. Wang, T. Jiang, X. Deng, S. Wei, Fabrication and abrasive wear property of high chromium cast iron with high vanadium and high nitrogen content (HCCI-VN). Wear **523**. 204828 (2023). DOI: https://doi.org/10.1016/j.wear.2023.204828

[6] R.H. Purba, K. Shimizu, K. Kusumoto, T. Todaka, M. Shirai, H. Hara, J. Ito, Erosive wear characteristics of high-chromium based multi-component white cast irons. Tribol. Int. **159**, 106982 (2021). DOI: https://doi.org/10.1016/j.triboint.2021.106982

[7] K. Shimizu, R.H. Purba, K. Kusumoto, X. Yaer, J. Ito, H. Kasuga, Y. Gaqi, Microstructural evaluation and high-temperature erosion characteristics of high chromium cast irons. Wear **426-427**, 420-427 (2019). DOI: https://doi.org/10.1016/j.wear.2019.01.043

[8] R.J. Chung, X. Tang, D.Y. Li, B. Hinckley, K. Dolman, Microstructure refinement of hypereutectic high Cr cast irons using hard carbide-forming elements for improved wear resistance. Wear **301** (1-2), 695-706 (2013). DOI: https://doi.org/10.1016/j.wear.2013.01.079

[9] R.J. Chung, X. Tang, D.Y. Li, B. Hinckley, K. Dolman, Effects of titanium addition on microstructure and wear resistance of hypereutectic high chromium cast iron Fe–25wt.%Cr–4wt.%C. Wear **267** (1-4), 356-361 (2009). DOI: https://doi.org/10.1016/j.wear.2008.12.061

[10] A. Bedolla-Jacuinde, R. Correa, J.G. Quezada, C. Maldonado, Effect of titanium on the as-cast microstructure of a 16%chromium white iron. Adv. Mater. Res-Switz. **398** (1-2), 297-308 (2005). DOI: https://doi.org/10.1016/j.msea.2005.03.072

[11] Ö.N. Doğan, J.A. Hawk, G. Laird, Solidification structure and abrasion resistance of high chromium white irons. Metall. Mater. Trans. A. **28** (6), 1315-1328 (1997). DOI: https://doi.org/10.1007/s11661-997-0267-3

[12] L. Laperrière, G. Reinhart, S. Chatti, T. Tolia (Ed), CIRP – The International Academy for Production Engineering, 2019 Springer, New York.

[13] Y. Gaqi, K. Kusumoto, K. Shimizu, R.H. Purba, Effect of Carbide Orientation on Wear Characteristics of High-Alloy Wear-Resistant Cast Irons. Lubricants **11** (7), 272 (2023). DOI: https://doi.org/10.3390/lubricants11070272

[14] M. Hashimoto, O. Kubo, Y. Matsuraba, Analysis of Carbides in Multi-component White Cast Iron for Hot Rolling Mill Rolls. Isij. Int. **44** (2), 372-380 (2004). DOI: https://doi.org/10.2355/isijinternational.44.372

[15] S. Ma, J. Xing, Y. He, Y. Li, Z. Huang, G. Liu, Q. Geng, Microstructure and crystallography of M_7C_3 carbide in chromium cast iron. Mater. Chem. Phys. **161**, 62-73 (2015). DOI: https://doi.org/10.1016/j.matchemphys.2015.05.008

[16] C. Tabrett, I.R. Sare, M.R. Ghomashchi, Microstructure-property relationships in high chromium white iron alloys. Int. Mater. Rev. **41** (2), 59-82 (1996). DOI: https://doi.org/10.1179/imr.1996.41.2.59

[17] C.M. Lin, H.H. Lai, J.C. Kuo, W. Wu, Effect of carbon content on solidification behaviors and morphological characteristics of the constituent phases in Cr-Fe-C alloys. Mater. Charact. **62** (12), 1124-1133 (2011). DOI: https://doi.org/10.1016/j.matchar.2011.09.007

[18] R.C. Touhami, S. Mechachti, K. Bouhamla, A. Hadji, A. Khettache, Wear Behavior and Microstructure Changes of a High Chromium Cast Iron: The Combined Effect of Heat Treatment and Alloying Elements. Metallogr. Microstruct. Anal. **12** (4), 580-590 (2023). DOI: https://doi.org/10.1007/s13632-023-00976-w

[19] S. Inditech, P. Sricharoenchai, Y. Masturaba, Effect of molybdenum content on subcritical heat treatment behaviour of hypoeutectic 16 and 26 wt-% chromium cast irons. Int. J. Cast. Metal. Res. **25** (5), 25-34 (2012). DOI: https://doi.org/10.1179/1743133612Y.0000000009

[20] S.O. Yilmaz, Wear behavior of gas tungsten arc deposited Fe-Cr-C, Fe-Cr-Si, and W-Co coatings on AISI 1018 steel. Surf. Coat. Technol. **194** (2-3), 175-183 (2005). DOI: https://doi.org/10.1016/j.surfcoat.2004.08.227

[21] X.H. Tang, R. Chung, C.J. Pang, D.Y. Li, B. Hinckley, K. Dolman, Microstructure of high (45wt.%) chromium cast irons and their resistances to wear and corrosion. Wear **271** (9-10), 1426-1431 (2011). DOI: https://doi.org/10.1016/j.wear.2010.11.047

[22] Nurbek Khamroev, Ilkhom Egamberdiev; Khisrav Ashurov; Sunnatullo Asatov; Boburjon Khamidov, Exploring the influence of the casting process, structural components and heat treatment on the mechanical properties of high-chromium cast irons: A review. AIP Conf. Proc. **3244**, 060021 (2024). DOI: https://doi.org/10.1063/5.0241423